ISSN 0031-918X, Physics of Metals and Metallography, 2020, Vol. 121, No. 8, pp. 804–810. © Pleiades Publishing, Ltd., 2020.
Russian Text © The Author(s), 2020, published in Fizika Metallov i Metallovedenie, 2020, Vol. 121, No. 8, pp. 884–891.

STRUCTURE, PHASE TRANSFORMATIONS, AND DIFFUSION

The Role of Deformation in Coagulation of $M_{23}C_6$ Carbide Particles in 9% Cr Steel

E. S. Tkachev[a], *, A. N. Belyakov[a], and R. O. Kaibyshev[a]

[a] *Belgorod State National Research University, Belgorod, 308015 Russia*

**e-mail: Tkachev_e@bsu.edu.ru*

Received January 22, 2020; revised February 12, 2020; accepted February 13, 2020

Abstract—The kinetics of the growth of $M_{23}C_6$ carbide particles in 9% Cr steel of the martensitic class with a high content of boron is studied under conditions of prolonged aging and creep. It is shown that the grain-boundary diffusion is a mechanism that controls the coagulation of these carbides in the case of annealing. Deformation accelerates the enlargement of particles during creep, which is explained by additional diffusion along dislocation lines.

Keywords: thermal engineering steel, particle growth mechanisms, creep behavior, structure

DOI: 10.1134/S0031918X20060162

INTRODUCTION

An increase in the boron content with a simultaneous decrease in the nitrogen content makes it possible to increase the operating temperatures of high chromium content steels of the martensitic class [1–8]. Using this approach to alloying, new thermal engineering steels MARBN, P93, and G115 for use as new-generation thermal engineering materials have been developed in Japan and China [3, 7]. It is known that the degradation of the initial lath structure of tempered troostite, which includes particle enlargement, depletion of the ferrite matrix by elements providing solid-solution strengthening, and a decrease in the density of intercrystalline boundaries due to the growth of the lath structure and its transformation into the subgrain structure are reasons for a decrease in the strength of high chromium content steels under creep conditions. The contribution of the particles of the second phases to the heat resistance is of particular importance, since they prevent the migration of lath/subgrain boundaries in addition to ensuring the dispersion strengthening, [1, 2, 5, 6, 8–11]. Kostka et al. [9] showed that the strengthening by particles of the second phases in martensitic steel leads to a decrease in the creep rate by more than two orders of magnitude.

At present, dispersion hardening in high chromium content steels is ensured by several types of particles ($M_{23}C_6$, Fe_2W, MX, Z-phase, etc.) with different morphologies, distributions, and growth rates [2, 5, 6, 9–12]. The introduction of MX carbonitride nanoparticles into 9% Cr steel made it possible to raise the operating temperature of these steels (P911 and P92) to 580–600°C [1, 10]. During the heat treatment, $M_{23}C_6$ carbide particles are released along the boundaries of the initial austenitic grains (IAGs), packs, blocks, and laths [2, 5, 6, 11, 12] and occupy the largest volume fraction among all types of particles. In high chromium content steels with a high content of boron, $M_{23}C_6$ carbide particles make it possible to raise the operating temperature to about 630°C, since they have a significant effect on the creep resistance. These particles play the role of obstacles for the movement of dislocations along the martensite laths and inhibit the redistribution of dislocations within the lath boundaries and the migration of boundaries. The initial size and the growth kinetics of these particles during creep determine the long-term strength in steels of the P93 type [2, 5, 6].

It has previously been established [2, 4–8, 13] that an increased boron content slows down the process of enlargement of $M_{23}C_6$ particles. It is believed that doping with boron leads to a decrease in the interfacial energy of $M_{23}C_6$ carbide, improves the stability against coagulation, and ensures structural stability due to the Zener pinning force [2, 5, 14, 15]. This increases the stability of the lath structure and improves the heat resistance characteristics [2, 4–8, 14, 16]. The positive effect of boron on the retardation of $M_{23}C_6$ carbide coagulation makes it possible to stabilize carbide particles located at the boundaries of laths and blocks, which is of fundamental importance for the long-term strength and helps to preserve the lath structure during long-term operation.

Dislocation creep in 9% Cr steels with an increased boron content at high temperatures (around 650°C) has a significant effect on the growth kinetics of $M_{23}C_6$

Table 1. Chemical composition of the steel under study, wt %

C	Si	Mn	Cr	W	Mo	Nb	V	Co	Ni	Cu	Ti	Al	N	B	Fe
0.1	0.12	0.4	9.0	1.5	0.57	0.05	0.2	2.8	0.24	0.027	0.002	0.01	0.007	0.012	Rest

particles, which is clearly seen when comparing the mean particle sizes in the regions of grips and working parts of samples tested for creep behavior [2, 4–6, 14]. Unfortunately, the mechanisms of coagulation of $M_{23}C_6$ carbide particles under creep conditions and the reasons for their accelerated growth under the influence of deformation have not been studied in detail.

In this study, we analyze the mechanism of enlargement of $M_{23}C_6$ carbide particles during annealing and under creep conditions in 9% Cr steel with a high boron content. A theoretical model is proposed that explains the change in the kinetics of growth of these particles under the influence of deformation during creep.

MATERIALS AND METHODS

The chemical composition of the steel used for the analysis is given in Table 1 [5, 6, 17]. The steel was smelted in a vacuum induction furnace and subjected afterwards to homogenizing annealing at a temperature of 1150°C and forged in the temperature range of 1150–1000°C. At the next stage, the finishing heat treatment (TH) was carried out, including normalization for 0.5 hours at 1060°C and subsequent tempering for 3 hours at 750°C.

An analysis of the phase composition and investigation of the fine structure were carried out by transmission electron microscopy (TEM) on a JEM-2100 microscope (Jeol, Japan) with an accelerating voltage of 200 kV. Foils were prepared using the method of double-sided jet electrochemical polishing on a Tenupol-5 device (Struers, Denmark). A 10% solution of $HClO_4$ in acetic acid was used as an electrolyte. To perform the phase analysis, carbon replicas were obtained from the samples, which were then studied by TEM. The phases were identified both by determining the chemical composition and by recording and interpreting electron diffraction patterns. To determine the mean particle size of the phases for each state, at least 300 measurements were performed.

The equilibrium volume fractions of carbides and the equilibrium concentration of Cr in the matrix, which were used in the particle growth equations, were calculated using the ThermoCalc software package with the TCFE7 database used for steels.

RESULTS AND DISCUSSION

The initial structure and distribution of dispersed particles of the second phases, and their evolution during prolonged aging and creep have been analyzed in detail in previous studies [5, 6, 17]. In this study, we note that the steel structure analyzed after heat treatment corresponds to tempered troostite with the inherited structure of lath martensite. The tempering led to a twofold decrease in the dislocation density; the size parameters of the martensite structure increased insignificantly [17]. Particles of carbide $M_{23}C_6$ are predominantly located at the boundaries of IAGs, packs, and blocks. Along the lath boundaries, such carbide particles are found more rarely; however, these particles play a key role in the creep resistance during long operating times [5]. Particles of (Nb, V)(C, N) carbonitrides are uniformly distributed in the ferrite matrix. In the intermediate stage of creep at 650°C, particles of the Fe_2(W, Mo) Laves phase are released along the boundaries of the structural elements; furthermore, a rather large number of them are released along the lath boundaries. With prolonged creep, the vast majority of $M_{23}C_6$ carbide and Laves phase particles located along the lath boundaries dissolve by the time the accelerated creep stage starts, which leads to the localization of plastic flows in the necked regions of the samples, in which the lath structure transforms into a subgrain structure [5]. The transformation of a small amount of carbonitrides into Cr(V, Nb)N nitride, known as the Z-phase [18], is observed only under creep conditions and leads to a significant increase in the particle size. Nevertheless, this reaction caused by deformation does not affect the long-term strength, which is likely associated with a small volume fraction of these particles in the steel under consideration [5].

The increased heat resistance of the studied steel compared to P92 steel additionally alloyed with 3% Co [1] is determined by a smaller size of $M_{23}C_6$ carbide particles (Fig. 1) [5–7, 12, 20], which provides a low creep rate in combination with the release of Laves phase particles along the lath boundaries in the established stage of creeping [5]. The dissolution of $M_{23}C_6$ particles located along the lath boundaries is observed in all 9–12% Cr steels upon an increase in the creep time [2, 5, 6, 11, 12, 20, 21]. Moreover, only those steels in which a sufficiently large number of $M_{23}C_6$ carbide particles remain along the lath boundaries under creep conditions exhibit the ultrahigh long-term strength [2, 5].

It should be noted that the release of $M_{23}C_6$ particles in steels with a high boron content does not stop during tempering [5, 21]. Subsequently, the specific volume of these carbide particles approaches to the thermodynamic equilibrium value at the creep temperature [5]. It was found that an increase in the vol-

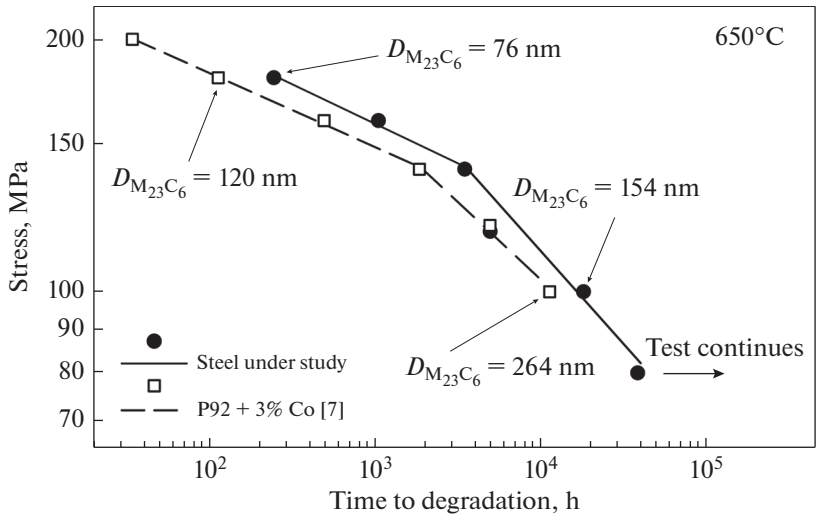

Fig. 1. Long-term strength curves for the steel under study and the P92–3% Co steel at 650°C.

ume fraction of particles during creep is determined by an increase in the size of $M_{23}C_6$ carbide particles without a significant increase in their number.

The rate of growth of $M_{23}C_6$ carbide particles is relatively low during long-term aging, which is associated with the low interfacial energy of these particles, especially in steels with a high content of boron [5, 21, 22]. Without changes caused by deformation in the distribution of particles of the second phases, high chromium content steels keep the lath structure unchanged for a long time [2, 5, 6, 11, 12, 20, 21]. However, the effect of deformation on creeping leads to a significant increase in the growth kinetics of particles of the second phases, in particular, $M_{23}C_6$ particles. Moreover, the mechanism of deformation-induced accelerated coagulation of $M_{23}C_6$ carbide particles has not been reliably established to date.

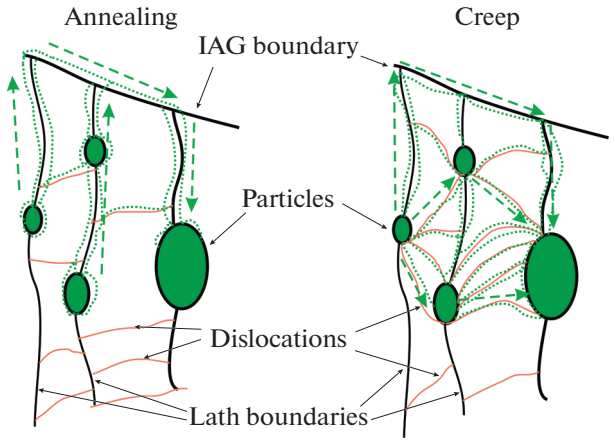

Fig. 2. Schematic picture illustrating the emergence of an additional diffusion influx to $M_{23}C_6$ particles upon changing the configuration of dislocations under the influence of creep deformation.

There are two possible reasons for the acceleration of coagulation of $M_{23}C_6$ carbide particles in consequence of creep deformation. First, deformation can lead to an increase in the interfacial energy due to the loss of coherence of the interface boundaries of $M_{23}C_6$ carbide particles [23, 24], which leads to an increase in their coagulation rate under creep conditions. Second, the additional diffusion flux along dislocation lines retained on $M_{23}C_6$ particles and various intergranular boundaries during sliding and/or crawling can be a reason for the accelerated growth of particles under creep conditions [2, 5, 6, 20, 21]. Dislocations accelerate coagulation for two reasons. First, if a dislocation connects an interfacial surface with a boundary or another particle, then an additional diffusion flux of alloying elements from a soluble particle to a growing one is produced, since the activation energy of pipe diffusion is much less than that of bulk diffusion (Fig. 2). Second, moving dislocations interact with the dissolved atoms of alloying elements through elastic interaction, which leads to the formation of atomic atmospheres along the dislocation core. At the same time, the alloying elements segregated on the dislocation core are transported by pipe diffusion to the particle, on which the dislocation is retained [25].

The enlargement of dispersed particles with the preservation of their volume fraction at the late stage of diffusion decay occurs through diffusion transfer of matter from smaller particles to larger ones and is called “Ostwald ripening”, a consistent theory of which was first constructed in [26, 27]. The kinetics of particle growth in each particular case depends on the prevailing mass transfer mechanism, which is the controlling one, as described in detail in [26–31]. The predominant arrangement of $M_{23}C_6$ particles along

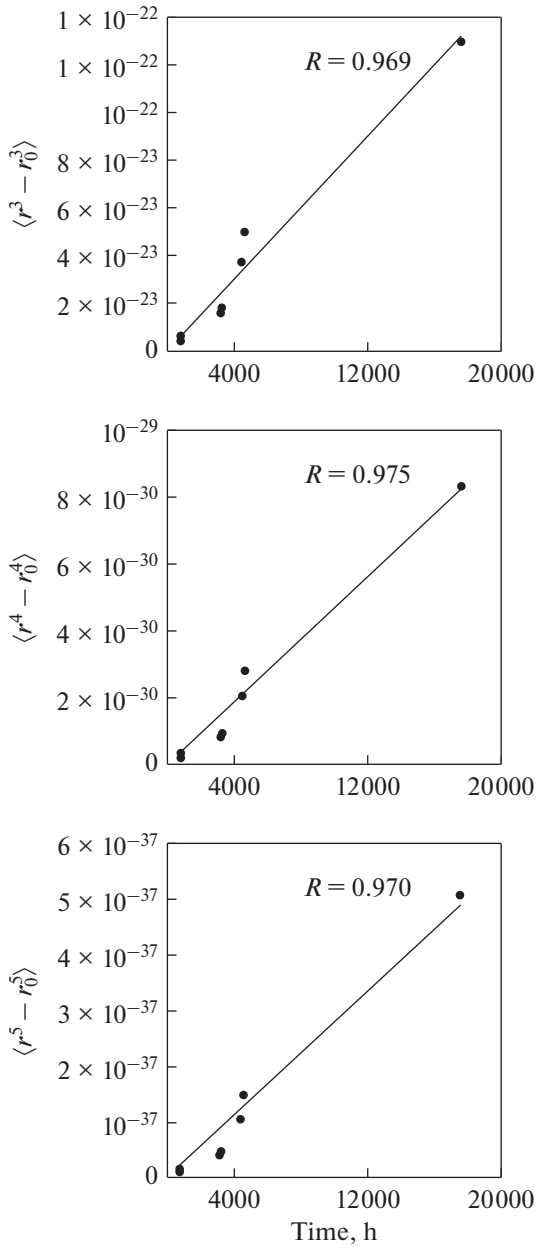

Fig. 3. Experimental data on the growth kinetics of $M_{23}C_6$ particles for n = 3, 4, 5 corresponding to bulk, grain-boundary, and pipe diffusion mechanisms, respectively.

the intercrystallite boundaries suggests that the grain-boundary diffusion is a controlling mass-transfer mechanism. To accurately determine the controlling mass-transfer mechanism, the experimental data were organized as a function of $r^n - r_0^n$ on the annealing time, where values n = 3, 4, 5 correspond to mass transfer controlled by bulk, grain-boundary, and pipe diffusion mechanisms, respectively (Fig. 3). The best agreement between the experimental data is observed for the $r^4 - r_0^4$ dependence, which confirms the grain-

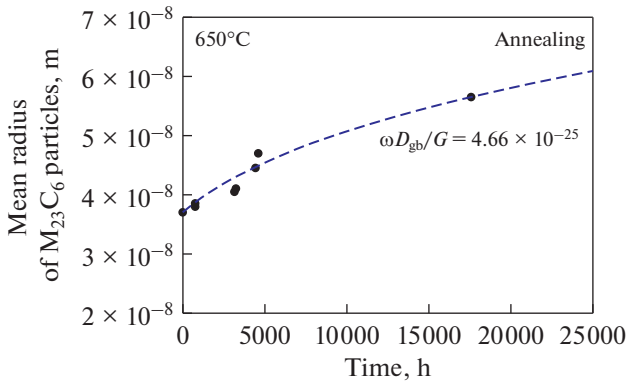

Fig. 4. Change in the mean radius of $M_{23}C_6$ particles during annealing of the steel under study. The dashed line shows the dependence calculated using Eqs. (1) and (2).

boundary mechanism of enlargement of $M_{23}C_6$ particles. In the case when the grain-boundary diffusion is a controlling mechanism, the change in the mean particle radius as a function of time is described as follows [28]:

$$\langle r\rangle^4 - \langle r_0\rangle^4 = K_{gb}t, \quad (1)$$

$$K_{gb} = \frac{8\gamma c_e D_{gb}\omega\Omega^2}{3GRT}\frac{u(\varphi)^4}{v(\varphi)}, \quad (2)$$

where γ is the interfacial energy, c_e is the equilibrium concentration of the element in the matrix, D_{gb} is the coefficient of grain-boundary diffusion with a width of ω, Ω is the molar volume of the phase, and $u(\varphi)$ and $v(\varphi)$ are the parameters depending on volume fraction φ of particles (Table 2). The dependence obtained using this equation describes well the observed changes in the particle size during annealing (Fig. 4).

However, the standard model of enlargement cannot explain the accelerated growth of particles under creep conditions. As mentioned earlier, the accelerated enlargement of particles under the influence of stress/strain can be caused either by an increase in the interfacial energy when their coherence is violated or by the appearance of additional paths for mass transfer.

The studies of the structure of the steel under consideration [5] did not reveal substantial differences in the orientational ratios of $M_{23}C_6$ particles with a ferritic matrix during annealing and creep. It can be concluded that creep does not lead to a significant change in the interfacial energy of these particles.

Figure 5 shows the dependence of the difference in the mean size of $M_{23}C_6$ particles during creep and annealing in comparison with the P92–3% Co steel.

As can be seen, the difference in the particle size changes during creep with approximately the same rate despite the significant difference in the mean size of particles, which points to the fact that a

Table 2. Parameters used in equations describing the enlargement of $M_{23}C_6$ particles in the steel under study

Parameter	Value	Reference
Interfacial energy, γ	0.12 J/m^2	[22]
Equilibrium concentration of Cr in matrix, c_e	11.79×10^3 mol/m^3	Calculated in ThermoCalc
Molar volume of $M_{23}C_6$, Ω	6.53×10^{-6} m^3/mol	Calculated in ThermoCalc
$\omega D_{gb}/G$	4.66×10^{-25} cm^2 s^{-1}	Adjusted value
Volume fraction of $M_{23}C_6$, φ	0.021670	Calculated in ThermoCalc
v	10.0	[28]
η	0.3	[28]
u	1.02	[28]
Coefficient of pipe diffusion, D_p	5.0×10^{-14} m^2 s^{-1}	[32]
Cross-sectional area of dislocation pipe, q	7.2×10^{-19} m^2	[32]

decrease in the interfacial energy does not have a significant effect on the accelerated enlargement caused by deformation.

It is known that the particle enlargement rate is proportional to the density of the diffusion flux of atoms directed toward the particle in accordance with the following formula:

$$\frac{dr}{dt} = \sum_i J_i, \tag{3}$$

where J_i is the diffusion flux density of the ith mass-transfer mechanism. In the case of bulk diffusion, the enlargement rate is defined as follows [26]:

$$r^2 \frac{dr}{dt} = \frac{8\gamma c_e D\Omega^2}{27RT} = K_V. \tag{4}$$

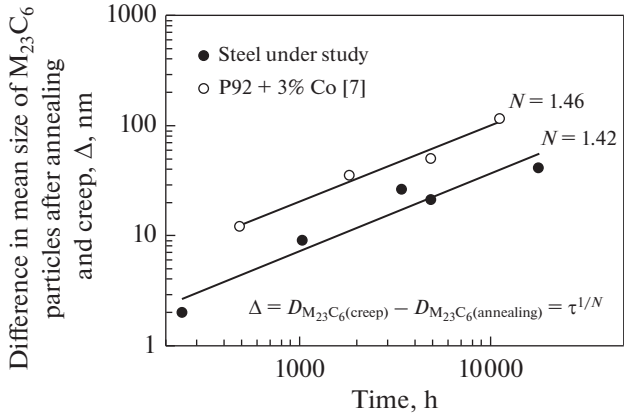

Fig. 5. Change in the difference in the mean size of $M_{23}C_6$ particles during creep and annealing in the steel under study compared to the P92–3% Co steel.

In accordance with the enlargement models proposed by Ardell [28], the enlargement rate under grain-boundary diffusion is

$$r^3 \frac{dr}{dt} = \frac{2\gamma c_e w D_{gb}\Omega^2}{3GRT} \frac{(u-1)}{\ln[(1+\eta u/\eta u]} = K_{GB}. \tag{5}$$

If mass transfer occurs along dislocations,

$$r^4 \frac{dr}{dt} = N \frac{q c_e D_p \Omega^2}{2\pi RT} \eta u (u-1) = N K_P, \tag{6}$$

where η and u are the parameters depending on volume fraction φ of particles (Table 2), N is the average number of dislocations in contact with each particle, and q is the cross-sectional area of the dislocation pipe.

To explain the difference in the kinetics of particle enlargement, we assume that the enlargement of $M_{23}C_6$ particles under creep conditions occurs under the simultaneous action of the grain-boundary and dislocation mass-transfer mechanisms, while the contribution of bulk diffusion to predicted times can be neglected. This assumption agrees well with the observed steel microstructure after creep (Fig. 6), in which many dislocations are in contact with particles located at different boundaries.

Based on the additivity of the particle growth rates, we can obtain the following equation combining the $t^{1/4}$ and $t^{1/5}$ dependences:

$$\frac{dr}{dt} = \frac{K_{GB}}{r^3} + \frac{\bar{N} K_P}{r^4}. \tag{7}$$

Equation (7) correctly describes the particle enlargement process in the case if the mass transfer takes place only along grain boundaries ($K_P = 0$) and dislocation pipes ($K_{GB} = 0$). Figure 7 shows the results of calculating the particle enlargement kinetics obtained using Eq. (7).

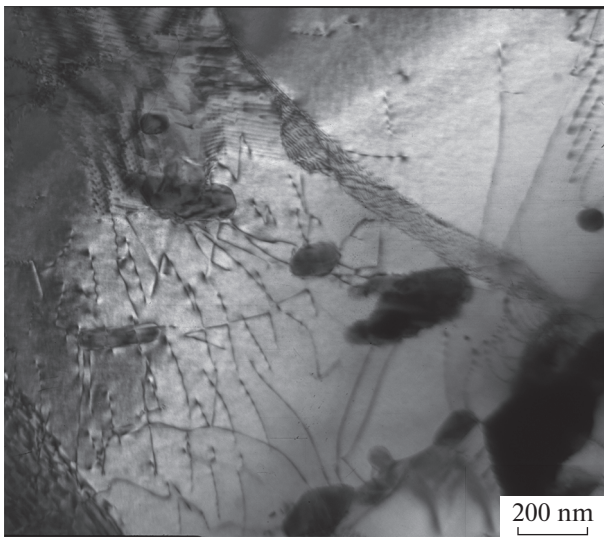

Fig. 6. Particles of $M_{23}C_6$ carbide in contact with many dislocations after 17 863 h of creep at 650°C.

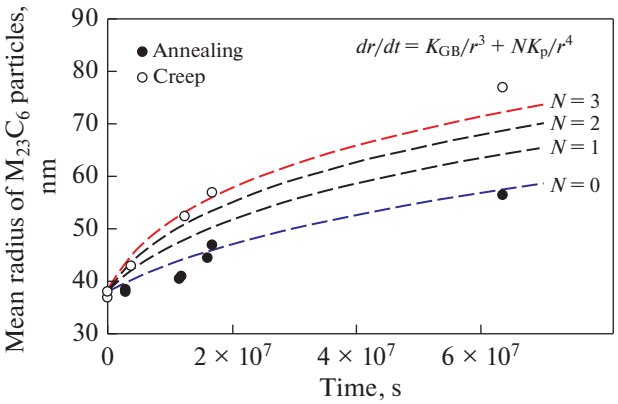

Fig. 7. Dependence of the mean radius of $M_{23}C_6$ particles on the annealing/creep time at 650°C in the steel under study. The dashed lines indicate the dependences obtained using Eq. (7).

In other words, the additional contribution of the diffusion flux from three dislocations on average to each particle at a constant value of the interfacial energy explains the observed difference in the kinetics of enlargement of $M_{23}C_6$ particles during annealing and creep. At the same time, it should be borne in mind that the given simplified model of particle enlargement for the mixed mass-transfer mechanism does not take into account the spread in particle sizes at the boundaries of various types in the initial state, as well as a change in the chemical composition of particles with an increase in the creep/annealing duration.

CONCLUSIONS

The kinetics of enlargement of $M_{23}C_6$ carbide particles during long-term annealing and creep in a martensitic steel containing 9% Cr was analyzed. It is established that alloying with boron does not have a significant effect on the acceleration of the enlargement of particles under the influence of creep deformation, despite a decrease in the initial size of particles and a decrease in their growth rate.

The accelerated enlargement of particles during creep can be explained by their interaction with dislocations, which leads to the simultaneous action of two mass-transfer mechanisms (grain-boundary diffusion and pipe diffusion) and can be generally described by an equation including the $t^{1/4}$ and $t^{1/5}$ dependences.

REFERENCES

1. R. O. Kaibyshev, V. N. Skorobogatykh, and I. A. Shchenkova, "New martensitic steels for fossil power plant: Creep resistance," Phys. Met. Metallogr. **109**, 186–200 (2010).
2. N. Dudova, R. Mishnev, and R. Kaibyshev, "Creep behavior of a 10% Cr heat-resistant martensitic steel with low nitrogen and high boron contents at 650°C," Mater. Sci. Eng., A **766**, 138353 (2019).
3. T. Matsunaga, H. Hongo, M. Tabuchi, M. Souissi, R. Sahara, C. Whitt, and M. J. Mills, "Creep lifetime and microstructure evolution in boron-added 9Cr–1Mo heat-resistant steel," Mater. Sci. Eng., A **760**, 267–276 (2019).
4. I. Fedorova, F. B. Grumsen, J. Hald, H. O. Andrén, and F. Liu, "Analyzing boron in 9–12% chromium steels using atom probe tomography," Microsc. Microanal. **25**, 462–469 (2019).
5. E. Tkachev, A. Belyakov, and R. Kaibyshev, "Creep strength breakdown and microstructure in a 9% Cr steel with high B and low N contents," Mater. Sci. Eng., A **720**, 138821 (2020).
6. E. Tkachev, A. Belyakov, and R. Kaibyshev, "Creep behavior and microstructural evolution of a 9% Cr steel with high B and low N contents," Mater. Sci. Eng., A **725**, 228–241 (2018).
7. F. Abe, *New Martensitic Steels, Materials for Ultra-Supercritical and Advanced Ultra-Supercritical Power Plants*, (Woodhead Publishing, 2017), pp. 323–374.
8. M. Akhtar, A. Khajuria, V. S. Kumar, R. K. Gupta, and S. K. Albert, "Evolution of microstructure during welding simulation of boron modified P91 steel," Phys. Met. Metallogr. **120**, 672–685 (2019).
9. A. Kostka, K. G. Tak, R. J. Hellmig, Y. Estrin, and G. Eggeler, "On the contribution of carbides and micrograin boundaries to the creep strength of tempered martensite ferritic steels," Acta Mater. **55**, 539–550 (2017).
10. V. V. Sagaradze, T. N. Kochetkova, N. V. Kataeva, K. A. Kozlov, V. A. Zavalishin, N. F. Vil'danova, V. S. Ageev, M. V. Leont'eva-Smirnova, and A. A. Nikitina, "Structure and creep of Russian reactor steels with a BCC structure," Phys. Met. Metallogr. **118**, 494–506 (2017).
11. Bori Yu. I. Borisova, V. A. Dudko, V. N. Skorobogatykh, I. A. Shchenkova, R. O. Kaibyshev, "Micro-

structural changes in cast martensitic steel after creep at 620°C," Phys. Met. Metallogr. **118**, 1022–1030 (2017).

12. A. E. Fedoseeva, N. R. Dudova, and R. O. Kaibyshev, "Effect of stresses on the structural changes in high-chromium steel upon creep," Phys. Met. Metallogr. **118**, 591–600 (2017).
13. R. Sahara, T. Matsunaga, H. Hongo, and M. Tabuchi, "Theoretical investigation of stabilizing mechanism by boron in body-centered cubic iron through $(Fe,Cr)_{23}(C,B)_6$ precipitates," Metall. Mater. Trans. A **47**, 2487–2497 (2016).
14. F. Abe, T. Horiuchi, M. Taneike, and K. Sawada, "Stabilization of martensitic microstructure in advanced 9Cr steel during creep at high temperature," Mater. Sci. Eng., A **378**, 299–303 (2004).
15. I. I. Gorbachev, A. Yu. Pasynkov, and V. V. Popov, "Prediction of the austenite grain size of microalloyed steels based on the simulation of the evolution of carbonitride precipitates," Phys. Met. Metallogr. **116**, 1127–1134 (2015).
16. G. Golański, A. Merda, and K. Klimaszewska, "Microstructural aspects of long-term ageing of martensitic 9% Cr steel with and without boron addition," J. Met. Mater. **71**, 27–33 (2019).
17. I. Fedorova, A. Kostka, E. Tkachev, A. Belyakov, and R. Kaibyshev, "Tempering behavior of a low nitrogen boron-added 9% Cr steel," Mater. Sci. Eng. A **662**, 443–455 (2016).
18. H. K. Danielsen, "Review of Z phase precipitation in 9–12 wt % Cr steels," Mater. Sci. Technol. **32**, 126–137 (2016).
19. A. Fedoseeva, I. Nikitin, N. Dudova, and R. Kaibyshev, "Strain-induced Z-phase formation in a 9% Cr–3% Co martensitic steel during creep at elevated temperature," Mater. Sci. Eng., A **724**, 29–36 (2018).
20. A. Fedoseeva, N. Dudova, and R. Kaibyshev, "Creep strength breakdown and microstructure evolution in a 3% Co modified P92 steel," Mater. Sci. Eng., A **654**, 1–12 (2016).
21. R. Mishnev, N. Dudova, and R. Kaibyshev, "On the origin of the superior long-term creep resistance of a 10% Cr steel," Mater. Sci. Eng., A **713**, 161–173 (2018).
22. A. Fedoseeva, E. Tkachev, V. Dudko, N. Dudova, and R. Kaibyshev, "Effect of alloying on interfacial energy of precipitation/matrix in high-chromium martensitic steels," J. Mater. Sci. **52**, 4197–4209 (2017).
23. A. Kipelova, A. Belyakov, and R. Kaibyshev, "The crystallography of $M_{23}C_6$ carbides in a martensitic 9% Cr steel after tempering, aging and creep," Philos. Mag. **93**, 2259–2268 (2013).
24. A. Deschamps and Y. Brechet, "Influence of predeformation and ageing of an Al–Zn–Mg Alloy. II Modeling of precipitation kinetics and yield stress," Acta Mater. **47**, 293–305 (1999).
25. T. Nakajima, S. Spigarelli, E. Evangelista, and T. Endo, "Strain enhanced growth of precipitates during creep of T91," Mater. Trans. **44**, 1802–1808 (2003).
26. I. M. Lifshits and V. V. Slezov, "On the kinetics of diffusion decay of supersaturated solid solutions," Zh. Eksp. Teor. Fiz. **35**, 479–492 (1958).
27. I. M. Lifshits and V. V. Slezov, "On the theory of coalescence of solid solutions," Fiz. Tverd. Tela **1**, 1401–1410 (1959).
28. A. Ardell, "On the coarsening of grain boundary precipitates," Acta Metall. **20**, 601–609 (1972).
29. R. D. Vengrenovich, A. V. Moskalyuk, and S. V. Yarema, "Ostwald ripening under conditions of mixed-type diffusion," Phys. Solid State **49**, 11–17 (2007).
30. V. V. Kondrat'ev and Yu. M. Ustyugov, "The kinetics of decomposition of supersaturated solid solutions with various mechanisms of mass transfer. I. Coalescence stage," Phys. Met. Metallogr. **76**, 433–439 (1993).
31. Yu. M. Ustyugov, "Decomposition of the supersaturated solid solutions at the stage of coalescence under conditions of passage from dislocation-controlled to volume diffusion," Phys. Met. Metallogr. **104**, 453–460 (2007).
32. H. Mehrer and M. Lübbehusen, "Self-diffusion along dislocations and in the lattice of alpha-iron," Defect Diffus. Forum, No. 66, 591–604 (1990).

Translated by O. Kadkin

SPELL: 1. ok